Journal of Solid State Chemistry 305 (2022) 122638

Contents lists available at ScienceDirect

Journal of Solid State Chemistry

journal homepage: www.elsevier.com/locate/jssc

Synthesis, crystal structures, and properties of new acentric glaserite-related compounds $Rb_7Ag_{5-3x}Sc_{2+x}(XO_4)_9$ (X = Mo, W)

Tatyana S. Spiridonova [a,*], Sergey F. Solodovnikov [b], Maxim S. Molokeev [c,d], Zoya A. Solodovnikova [b], Aleksandra A. Savina [a,e], Yulia M. Kadyrova [a], Aleksandr S. Sukhikh [b], Evgeniy V. Kovtunets [a], Elena G. Khaikina [a]

[a] Baikal Institute of Nature Management, Siberian Branch, Russian Academy of Sciences, Sakh'yanova St. 6, Ulan-Ude, 670047, Buryat Republic, Russian Federation
[b] Nikolaev Institute of Inorganic Chemistry, Siberian Branch, Russian Academy of Sciences, Akad. Lavrentyev Ave. 3, Novosibirsk 630090, Russian Federation
[c] Kirensky Institute of Physics, Federal Research Center KSC SB RAS, Akademgorodok 50 bld.38, Krasnoyarsk, 660036, Russian Federation
[d] Kemerovo State University, Krasnaya St., 6, Kemerovo, 650000, Russian Federation
[e] Skolkovo Institute of Science and Technology, Moscow, 121205, Russian Federation

ARTICLE INFO

Keywords:
Rubidium
Silver
Scandium
Triple molybdate
Triple tungstate
Phase equilibria
Synthesis
Crystal structure
Ionic conductivity

ABSTRACT

The subsolidus phase equilibria in the system Ag_2MoO_4–Rb_2MoO_4–$Sc_2(MoO_4)_3$ were studied and two new triple molybdates, $Rb_9Ag_3Sc_2(MoO_4)_9$ and $Rb_7Ag_5Sc_2(MoO_4)_9$, were found. The structures of $Rb_7Ag_5Sc_2(MoO_4)_9$ and isostructural $Rb_7Ag_5Sc_2(WO_4)_9$ of the $Cs_7Na_5Yb_2(MoO_4)_9$ type (the space group $R32$) were determined. The found composition of the triple tungstate crystal, $Rb_7Ag_{4.61}Sc_{2.13}(WO_4)_9$, indicates a non-stoichiometric compound formula, $Rb_7Ag_{5-3x}Sc_{2+x}(WO_4)_9$. Both structures have one incompletely occupied Ag site, and structure $Rb_7Ag_{4.61}Sc_{2.13}(WO_4)_9$ also contains two positions with mixed Ag and Sc. Both compounds contain 'lanterns' $[M_2(XO_4)_9]$ (M = (Sc, Ag), Sc; X = Mo, W), which are strengthened by three AgO_2 dumbbells to give isolated building blocks $[Ag_3M_2(XO_4)_9]$ forming two-story hexagonal layers resembling the structure of glaserite $K_3Na(SO_4)_2$. Similar layers of $[Ag_3Sc_2(WO_4)_9]^{9-}$ building blocks were also found by us in the structure of $Rb_{9-x}Ag_{3+x}Sc_2(WO_4)_9$, which is close to that of $Rb_9Ag_3Sc_2(MoO_4)_9$. Similar layers of the $[M_2(TO_4)_9]$ units were also observed in $Cs_7Na_5Yb_2(MoO_4)_9$ and $Na_{13}Sr_2Ta_2(PO_4)_9$. The title compounds belong to the series of rhombohedral triple molybdates and tungstates with $a \approx 9$–10 Å and large c-periods (more than 20 Å), which have layered or open 3D framework structures. Like many compounds of this series, $Rb_7Ag_5Sc_2(XO_4)_9$ (X = W, Mo) at elevated temperatures have significant ionic conductivity reaching values $6.1{\cdot}10^{-3}$ S cm^{-1} at 703 K (X = Mo) and $1.4{\cdot}10^{-3}$ S cm^{-1} at 733 K (X = W) with E_a = 0.7 eV and 0.6 eV, respectively.

1. Introduction

Scandium tungstate, $Sc_2(WO_4)_3$, is the parent for a large family of compounds with negative thermal expansion (NTE) and also attracts attention by ionic conductivity with both oxygen-ions and WO_4^{2-} polyanions as carriers [1–3]. Scandium molybdate, $Sc_2(MoO_4)_3$, crystallizing in the $Sc_2(WO_4)_3$ structure type above 178 K [4] is also characterized by NTE [5]. In addition, microcrystals of $Sc_2Mo_3O_{12}$:Ln^{3+} (Ln = Tb, Eu, Tb/Eu, Yb/Er, Yb/Ho, Yb/Tm) show great potential applications in the areas of fluorescent lamps and color displays [6].

Complex scandium-containing tungstates and molybdates with two or three cations and mixed anions are also of great interest. Many of those are known or promising compounds as ferroelastics and piezoelectrics [7–9], materials with NTE [10,11], phosphors, laser host materials [10–14], ionic conductors [15–24], etc. Ferroelastic phase transitions were mainly found in double molybdates and tungstates of scandium and alkali metals with 1: 1 composition [7], which belong to trigonal KAl(MoO_4)$_2$ [25] at room temperature. Mixed-anion phases MSc$(WO_4)_2(PO_4)$ (M = Zr, Hf) of the $Sc_2(WO_4)_3$ type are found to show intense intrinsic luminescence in the visible spectral region at room temperature, and NTE improves their application as materials of light-emitting devices [10,11]. Triple molybdate $K_{0.6}(Mg_{0.3}Sc_{0.7})_2(MoO_4)_3$:$Cr^{3+}$ of the NASICON type

* Corresponding author.
E-mail addresses: spiridonova-25@mail.ru (T.S. Spiridonova), solod@niic.nsc.ru (S.F. Solodovnikov), msmolokeev@mail.ru (M.S. Molokeev), zoya@niic.nsc.ru (Z.A. Solodovnikova), a.savina@skoltech.ru (A.A. Savina), yliychem@yandex.ru (Y.M. Kadyrova), a_sukhikh@niic.nsc.ru (A.S. Sukhikh), kovtunets@gmail.com (E.V. Kovtunets), egkha@mail.ru (E.G. Khaikina).

https://doi.org/10.1016/j.jssc.2021.122638
Received 10 August 2021; Received in revised form 4 October 2021; Accepted 4 October 2021
Available online 14 October 2021

[26] is a potential laser material [12], while isostructural $K_{1-x}Mg_{1-x}Sc(Lu)_{1+x}(MoO_4)_3:Eu^{3+}$ may be promising in the development of WLED [13]. According to Ref. [14], $LiZnSc(MoO_4)_3:Eu^{3+}$ of the α-$ZnMoO_4$ type [27] can also be considered as a bright red phosphor.

The most numerous is the group of compounds with open framework structures, which have a high ionic conductivity. First of all, it is $M_{1-x}Mg_{1-x}Sc_{1+x}(MoO_4)_3$ (M = Na, Ag, K) of the NASICON type [15–18]; $Na_{25}Cs_8Sc_5(MoO_4)_{24}$ [19] and $Na_5Sc(MoO_4)_4$ [20], structurally related to alluaudite (Na, Ca)(Fe,Mn,Mg)$_3$(PO$_4$)$_3$ [28]; $Na_9Sc(MoO_4)_6$ [21] isostructural to sodium-ion conductor II-$Na_3Fe_2(AsO_4)_3$ [29], as well as $K_5ScZr(MoO_4)_6$ и $K_5ScHf(MoO_4)_6$ [22,23], belonging to the structure types of $Rb_5FeHf(MoO_4)_6$ [30] and $K_5InHf(MoO_4)_6$ [31], respectively. Our previous work reported on synthesis and study of triple tungstate $Rb_9Ag_3Sc_2(WO_4)_9$, which forms a new structure type [24]. Our theoretical analysis based on bond valence sum (BVS) calculations showed a possible two-dimensional rubidium-ion conductivity in $Rb_9Ag_3Sc_2(WO_4)_9$. This conclusion was confirmed experimentally and found that it is comparable with those of three-dimensional transport of rubidium ions in $RbNbWO_6$ of the defect pyrochlore type [32].

As a part of our work on searching for new ternary scandium-containing molybdates and tungstates, here we present the data on phase formation in the Ag_2MoO_4–Rb_2MoO_4–$Sc_2(MoO_4)_3$ system, identification, and characterization of one of the two triple molybdates formed in it, $Rb_7Ag_5Sc_2(MoO_4)_9$, along with its tungstate analog $Rb_7Ag_5Sc_2(WO_4)_9$.

2. Experimental

2.1. Preparation of materials

Commercially available chemically pure MoO_3, WO_3 (ReaKhim, Ltd, Russia), $AgNO_3$ (KhimKo, Ltd, Russia) and high purity Sc_2O_3 (SibMetallTorg, Ltd, Russia), Rb_2CO_3 (Sigma-Aldrich, China) were used as starting materials for preparing molybdates and tungstates. Compounds were synthesized in porcelain crucibles with thorough daily manual grindings of the starting reagents and reaction mixtures while annealing. Rb_2XO_4 (X = Mo, W) was prepared by firing a stoichiometric mixture of Rb_2CO_3 and XO_3 (723–823 K, 80 h). $Sc_2(XO_4)_3$ (X = Mo, W) was obtained from Sc_2O_3 and XO_3 (X = Mo, 773–1023 K, 80 h; X = W, 773–1123 K, 80 h). Both silver molybdate and tungstate were obtained by stepwise annealing of stoichiometric mixtures of $AgNO_3$ and XO_3 (X = Mo, W) at 623–773 K (X = Mo), 623–823 K (X = W) for 60 h. Double molybdates $AgRb_3(MoO_4)_2$, $Rb_5Sc(MoO_4)_4$ and $RbSc(MoO_4)_2$ for studying the Ag_2MoO_4–Rb_2MoO_4–$Sc_2(MoO_4)_3$ system was also prepared by solid-state reactions from stoichiometric mixtures of the corresponding simple molybdates at 653–723 K for 80–100 h.

The phase purity of the prepared samples was confirmed by powder X-ray diffraction (PXRD). The PXRD patterns of Ag_2XO_4, Rb_2XO_4, $Sc_2(XO_4)_3$ (X = Mo, W), $Rb_5Sc(MoO_4)_4$, $RbSc(MoO_4)_2$, and $Rb_3Ag(MoO_4)_2$ were in accordance with the literature data [33–35].

Small single crystals of the title compounds were grown by spontaneous crystallization of melts. For this, the heating of ground mixtures, the isothermal holding, and the slow cooling of the resulting melts were controlled automatically with an accuracy of ±0.5°.

2.2. Instrumental characterization methods

Processes of solid-state synthesis and phase equilibration were monitored with diffractograms taken with a D8 ADVANCE Bruker diffractometer (VANTEC detector, CuK_α radiation, λ = 1.5418 Å, reflection geometry, secondary monochromator). PXRD data were collected at 296 K over the range 2θ = 7–100°, with a step of 0.02076°.

The Rietveld refinement was carried out with the TOPAS 4.2 software [36].

Single-crystal XRD data for structure analysis of the title triple tungstate were collected at room temperature using a Bruker DUO diffractometer (MoK_α radiation, graphite monochromator, APEX II CCD detector). Data collection strategy consisted of single 360° φ-scan with a scan step of 0.5°. APEX3 V2018.7–2 software package (SAINT V8.38A, SADABS-2016/2) [37] was used for raw data processing, absorption correction and global unit cell refinement. The obtained *hkl* were processed in Olex2 v.1.2.10 software [38] using SHELXT-2018/2 [37] and SHELXL-2018/3 [39] for initial structure solution and subsequent refinement, respectively. Data processing was accomplished using SAINT program; an absorption correction was applied with SADABS program [39]. The structures were solved by means of direct methods with SHELXS and refined with SHELXL2017/1 program [40].

The refinement data for both crystal structures can be obtained from the Fachinformationszentrum Karlsruhe, 76344 Eggenstein-Leopoldshafen, Germany, (fax (+49)7247-808-666; e-mail: crysdata@fiz.karlsruhe.de, http://www.fiz-karlsruhe.de/request): on quoting the depository number CSD 2100936–2100937.

Thermoanalytical studies were carried out on an STA 449 F1 Jupiter NETZSCH thermoanalyser (Pt crucible, heating rate of 10 K min^{-1} in an argon stream).

Second harmonic generation (SHG) tests were performed with a laser system in reflection geometry using fine powders, as described in Refs. [41,42]. The optical nonlinearity of the materials was evaluated relative to an α-quartz reference (polycrystalline α-SiO_2 with 3–5 mm particle size), i.e. $I_{2\omega}/I_{2\omega}(SiO_2)$.

For studying the electrical conductivity, the ceramic disks of $Rb_7Ag_5Sc_2(XO_4)_9$ (X = Mo, W) were prepared by pressing the powder at 1 kbar and sintering at 723 (X = Mo) or 753 K (X = W) for 4 h. The density of the obtained disks of 10 mm in diameter and 1.8 mm thick was 90–95% of theoretical values. For preparing the electrode, the disk surface was coated with colloidal platinum, followed by annealing for 1 h. The electrical conductivity was measured by the two-contact method (impedance meter Z-1500J, temperature range of 473–723 K (X = Mo) and 473–743 K (X = W), heating and cooling rates of 2 deg/min). The activation energy values were calculated from the slope of the straight lines corresponding to the Arrhenius dependence in lg(σT) – (10^3/T) coordinates.

3. Results and discussion

3.1. Subsolidus phase relations in the Ag_2MoO_4–Rb_2MoO_4–$Sc_2(MoO_4)_3$ system

The quasi-binary system Ag_2MoO_4–Rb_2MoO_4 being a boundary element of the ternary system Ag_2MoO_4–Rb_2MoO_4–$Sc_2(MoO_4)_3$ was studied in our previous work [35]. We found the only compound $AgRb_3(MoO_4)_2$ of the glaserite, $K_3Na(SO_4)_2$, type [43], which melts at 708 K.

Since no data on studying the system Rb_2MoO_4–$Sc_2(MoO_4)_3$ in a wide concentration region were found in the literature, we investigated it with PXRD. The reaction mixtures containing 90, 83.3, 78, 75, 70, 65, 60, 50, and 25 mol% rubidium molybdate were calcined at 573–773 K by a step of 50 K and studied with PXRD. In this temperature range, this system was found to be quasi-binary and characterized by the formation of the known double molybdates $Rb_5Sc(MoO_4)_4$ and $RbSc(MoO_4)_2$ [34,44–51] with the structures related to those of palmierite $K_2Pb(SO_4)_2$ [52] and $KAl(MoO_4)_2$ [25], respectively.

A complete study of the Ag_2MoO_4–$Sc_2(MoO_4)_3$ system has also not been performed previously. Double molybdate $AgSc(MoO_4)_2$ [53] has no polymorphism, crystallizes in the $NaIn(MoO_4)_2$ structure [54], and decomposes in the solid phase at 803 K [53]. The authors of [53] did not obtain $AgSc(MoO_4)_2$ using solid-state reactions, although it was synthesized by precipitation from aqueous solutions followed by calcination at 723 K [53]. Our attempts to prepare $AgSc(MoO_4)_2$ and other double molybdates in the Ag_2MoO_4–$Sc_2(MoO_4)_3$ system by solid-state synthesis were also unsuccessful. According to our PXRD data, only the initial Ag_2MoO_4 and $Sc_2(MoO_4)_3$ were in the annealed samples.

Taking into account the literature and our data on binary boundary systems, the subsolidus phase equilibria in the system Ag_2MoO_4–Rb_2MoO_4–$Sc_2(MoO_4)_3$ was studied at 623–723 K (a step of 20–50 K) with the "intersecting joins" method [55,56] elaborated for the ternary systems with binary compounds in the boundary systems. In order to determine the quasi-binary joins in the ternary system and its triangulation, need to know the phase compositions of the annealed samples corresponding to the intersection points of the joins originating from the composition points of all components and binary compounds of the system. In addition, we also used the joins originating from hypothetical phases, real analogs of which were found in similar systems.

Thus, the subsolidus phase equilibria and compositions of the triple molybdates formed in the system Ag_2MoO_4–Rb_2MoO_4–$Sc_2(MoO_4)_3$ were determined (Fig. 1). Subsolidus interaction in the considered system leads to two triple molybdates $Rb_7Ag_5Sc_2(MoO_4)_9$ and $Rb_9Ag_3Sc_2(MoO_4)_9$. According to PXRD data, the first compound is isoformular and isostructural to $Cs_7Na_5Yb_2(MoO_4)_9$ described in our previous work [57]. The second compound $Rb_9Ag_3Sc_2(MoO_4)_9$ is at the intersection point of the joins $AgRb_3(MoO_4)_2$–$Sc_2(MoO_4)_3$ and «$AgRbMoO_4$»–«$Rb_3Sc(MoO_4)_3$».

The subsolidus phase equilibria in the system Ag_2MoO_4–Rb_2MoO_4–$Sc_2(MoO_4)_3$ are described by nine quasi-binary joins S_2–$AgRb_3(MoO_4)_2$, $AgRb_3(MoO_4)_2$–$Rb_5Sc(MoO_4)_4$, S_2–$Rb_5Sc(MoO_4)_4$, S_2–$RbSc(MoO_4)_2$, S_1–$RbSc(MoO_4)_2$, S_1–S_2, S_1–$AgRb_3(MoO_4)_2$, Ag_2MoO_4–S_1, Ag_2MoO_4–$RbSc(MoO_4)_2$, which divide the concentration triangle into eight secondary ones (Fig. 1). Noteworthy, the PXRD patterns of the samples in the concentration area Ag_2MoO_4–$RbSc(MoO_4)_2$–$Sc_2(MoO_4)_3$ contain no reflections of $AgSc(MoO_4)_2$.

The formation of isoformular triple tungstate $Rb_9Ag_3Sc_2(WO_4)_9$, its crystal structure and properties were reported in our previous work [24]. Similar diffractograms of $Rb_9Ag_3Sc_2(XO_4)_9$ (X = Mo, W) suggests their isostructurality or close structural relationship, but our attempts to perform the Rietveld refinements of the $Rb_9Ag_3Sc_2(MoO_4)_9$ structure gave no unambiguous results yet. A new triple tungstate $Rb_7Ag_5Sc_2(WO_4)_9$ isotypic with $Rb_7Ag_5Sc_2(MoO_4)_9$ was obtained by targeted solid-state synthesis.

This paper reports the data on synthesis, crystal structure determination, and some physicochemical properties of $Rb_7Ag_5Sc_2(XO_4)_9$ (X = Mo, W). The results of studying $Rb_9Ag_3Sc_2(MoO_4)_9$ will be published later.

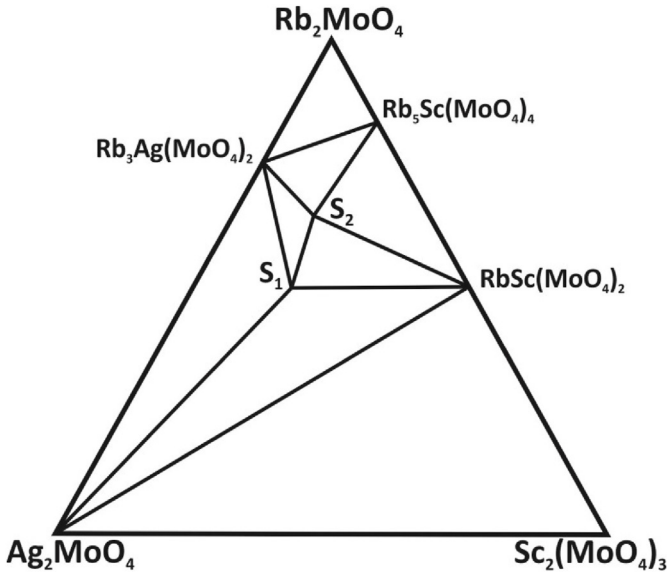

Fig. 1. Subsolidus phase relations in the Ag_2MoO_4–Rb_2MoO_4–$Sc_2(MoO_4)_3$ system at 723 K;
S_1–$Rb_7Ag_5Sc_2(MoO_4)_9$; S_2–$Rb_9Ag_3Sc_2(MoO_4)_9$.

3.2. Synthesis, crystal growth and characterization of $Rb_7Ag_5Sc_2(XO_4)_9$ (X = Mo, W)

Polycrystalline $Rb_7Ag_5Sc_2(XO_4)_9$ (X = Mo, W) were synthesized by annealing the stoichiometric mixtures of Ag_2XO_4, Rb_2XO_4 and $Sc_2(XO_4)_3$ at 673–723 K for 60–80 h (X = Mo), 723–743 K for 80–100 h (X = W). The final powder products of white color are insoluble in water and usual organic solvents, soluble in the dilute HCl, as well as in the concentrated and dilute HNO_3.

According to the PXRD data (Fig. 2), the sequence of chemical transformations with formation of $Rb_7Ag_5Sc_2(MoO_4)_9$ from a stoichiometric mixture of simple molybdates can be illustrated by the following scheme:

$$\left.\begin{matrix}Ag_2MoO_4\\Rb_2MoO_4\\Sc_2(MoO_4)_3\end{matrix}\right\} \xrightarrow{523\text{–}573\ K,\ 100\ h} \left.\begin{matrix}Ag_2MoO_4\\Rb_2MoO_4\\Sc_2(MoO_4)_3\\AgRb_3(MoO_4)_2\end{matrix}\right\} \xrightarrow{623\ K,\ 50\ h}$$

$$\xrightarrow{623\ K,\ 50\ h} \left.\begin{matrix}Ag_2MoO_4\\RbSc(MoO_4)_2\\Rb_9Ag_3Sc_2(MoO_4)_9\end{matrix}\right\} \xrightarrow{673\text{–}723\ K,\ 80\ h} Rb_7Ag_5Sc_2(MoO_4)_9$$

$Rb_7Ag_5Sc_2(WO_4)_9$ also forms through the stage of $Rb_9Ag_3Sc_2(WO_4)_9$ synthesis. The corresponding schemes differ from those of triple molybdate only in higher temperatures of the syntheses.

$Rb_7Ag_5Sc_2(XO_4)_9$ (X = Mo, W) are found to melt incongruently at 777 K (X = Mo) and 782 K (X = W). The reflections of Ag_2MoO_4, Rb_2MoO_4, $RbSc(MoO_4)_2$ and $Rb_9Ag_3Sc_2(MoO_4)_9$ were found on the diffractogram of a cooled melt of $Rb_7Ag_5Sc_2(MoO_4)_9$ along with the initial phase, whereas the PXRD pattern of molten and cooled $Rb_7Ag_5Sc_2(WO_4)_9$ shows a mixture of $AgWO_4$, $RbSc(WO_4)_2$ and an unidentified phase.

Crystallization runs for obtaining crystals of $Rb_7Ag_5Sc_2(XO_4)_9$ (X = Mo, W) suitable for structure determination gave a positive result only for the triple tungstate. Its colorless crystals were obtained by spontaneous crystallization of the molten sample with a nominal composition $Rb_5Ag_4Sc(WO_4)_6$. According to single-crystal structure analysis (see below), the composition of the studied crystal of the triple tungstate was found to be nonstoichiometric, $Rb_7Ag_{4.61}Sc_{2.13}(WO_4)_9$. It should be noted that single-phase sample $Rb_7Ag_{4.61}Sc_{2.13}(WO_4)_9$ was not prepared by the solid-state synthesis. After annealing of reaction

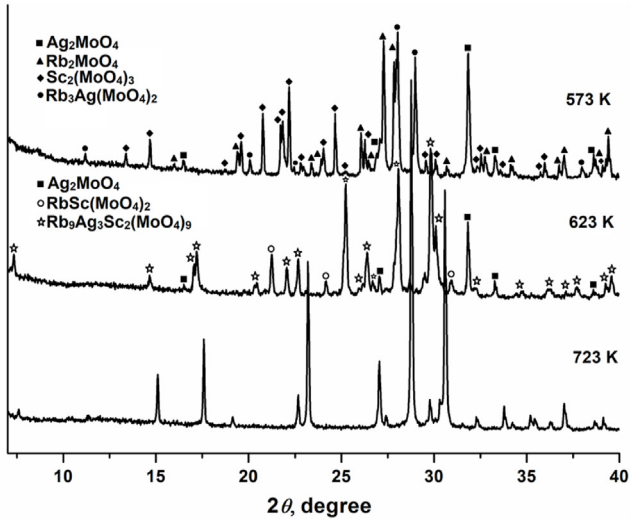

Fig. 2. Diffractograms of the mixture 5 Ag_2MoO_4 + 7 Rb_2MoO_4+ 2 $Sc_2(MoO_4)_3$ with stepwise heat treatment.

mixtures of silver, rubidium, and scandium molybdates or tungstates corresponding to the nominal compositions $Rb_7Ag_{5-3x}Sc_{2+x}(XO_4)_9$, X = Mo, W (x = 0, 0.1, 0.15, 0.2, 0.33) only samples with x = 0 were found single-phase even at highest subsolidus temperatures. The found composition of the studied crystal seems to have almost lowest silver content, which can be reached only with the melt crystallization. Nevertheless, the PXRD pattern of $Rb_7Ag_5Sc_2(WO_4)_9$ sample (Fig. 3) agree well with a theoretical diffractogram calculated from the X-ray structure analysis data, that indicates the phase purity of the obtained compound.

3.3. Crystal structure of $Rb_7Ag_{4.61}Sc_{2.13}(WO_4)_9$

The structure of $Rb_7Ag_{4.61}Sc_{2.13}(WO_4)_9$ was solved in the chiral sp. gr. $R32$ and refined taking into account the statistical distribution of the Ag^+ and Sc^{3+} cations over their positions provided that the structure is electrically neutral. These cations distribute over crystallographic positions in the following way: $Rb_7(Ag_{0.69}Sc_{0.31})(Sc_{0.91}Ag_{0.09})_2(Ag_{0.37})_2Ag_3(WO_4)_9$. In isostructural triple molybdate $Cs_7Na_5Yb_2(MoO_4)_9$ [55], the Na^+ and Yb^{3+} ions are located in similar positions as follows: $Cs_7NaYb_2(Na_{0.5})_2Na_3(MoO_4)_9$, that in principle also allows the nonstoichiometry of this compound due to a possible (Na, Yb) aliovalent substitution. Crystal and X-ray analysis data for $Rb_7Ag_{4.61}Sc_{2.13}(WO_4)_9$ are summarized in Table 1, and atomic coordinates, equivalent isotropic displacement parameters and selected interatomic distances are listed in Tables 1S and 2S of the supporting information.

In the structure of $Rb_7Ag_{4.61}Sc_{2.13}(WO_4)_9$, the atoms (Ag,Sc)1 and Ag3 are in threefold special positions with the point symmetry 32; (Sc,Ag)2, Rb1, and Rb2 sit at threefold axes; Rb3, W2, and Ag4 locate at twofold axes, and W1 and oxygen atoms are in 18-fold general positions. The W atoms have a usual slightly distorted tetrahedral coordination with the distances W–O 1.749(7)–1.815(8) Å, which are close to those in the structures of $Sc_2(WO_4)_3$ [4], $Rb_{9-x}Ag_{3+x}Sc_2(WO_4)_9$ [24] and other tungstates. The atoms (Ag,Sc)1 and (Sc,Ag)2 have nearly regular octahedral environments with the bond lengths (Ag,Sc)1–O1 2.418(10) Å (× 6) and (Sc,Ag)2–O 2.077(9)–2.118(9) Å. Interestingly, the Na1 atom in the structure of $Cs_7Na_5Yb_2(MoO_4)_9$ [58], which is similar in arrangement to (Ag,Sc)1, has a trigonal-prismatic coordination rather than an octahedral one. The partially occupied Ag3 site with the distances Ag3–O 2.442(10)–2.612(9) Å has a trigonal-prismatic environment, as does the half-occupied Na2 site in $Cs_7Na_5Yb_2(MoO_4)_9$. The bond lengths found for the mentioned sites with the Sc^{3+} and Ag^+ cations agree well with typical distances Sc–O 2.03–2.12 Å for ScO_6 octahedra found, for example, in the structures of $Sc_2(WO_4)_3$ [4], $Na_9Sc(MoO_4)_6$ [21], $Rb_{9-x}Ag_{3+x}Sc_2(WO_4)_9$ [24], $RbSc(MoO_4)_2$ [51], as well as with

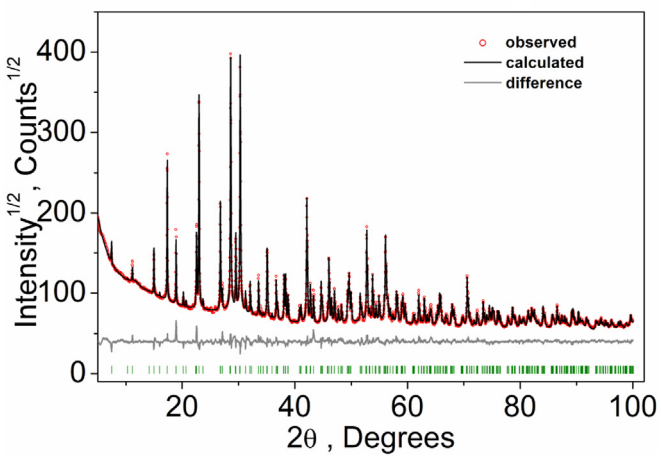

Fig. 3. Observed, calculated and difference diffractograms of $Rb_7Ag_5Sc_2(WO_4)_9$.

Table 1
Crystal data and structure refinement details for $Rb_7Ag_{4.61}Sc_{2.13}(WO_4)_9$.

Formula weight (g/mol)	3421.99
Crystal system	Trigonal
Space group	$R32$
Unit cell dimensions	a = 10.2031(4) Å, c = 35.4271(14) Å
V (Å^3)	3194.0(3)
Calculated density (g cm^{-3})	5.337
Formula units, Z	3
Absorption coefficient (mm^{-1})	34.616
Crystal size (mm)	0.06 × 0.04 × 0.03
Color	Colorless
2θ range (°)	4.752–61.11
Miller index ranges	$-14 \le h \le 14$, $-10 \le k \le 14$, $-50 \le / \le 44$
Reflections collected/unique	10093/2187 [R(int) = 0.0629]
Data/restraints/parameters	2188/1/97
Goodness-of-fit on F^2 (GOF)	0.999
Extinction coefficient	None
Final R indices [$I > 2\sigma(I)$]	$R(F)$ = 0.0323, w$R(F^2)$ = 0.0547
R indices (all data)	$R(F)$ = 0.0400, w$R(F^2)$ = 0.0565
Absolute structure (Flack) parameter	−0.016(12)
Largest difference peak/hole (e Å^{-3})	1.79/−1.56

Ag–O 2.30–2.80 Å for octahedral and trigonal prismatic coordinations of silver, which were found in $Ag_2M_2(MoO_4)_3$ (M = Co, Mn) [58], $Ag_4Mn_2Zr(MoO_4)_6$ [59] and $Rb_2AgIn(MoO_4)_3$ [60]. The shortest bond lengths Ag4–O3 2.192(9) Å (× 2) and the angle O3–Ag–O3' 171.9(6)° determine a nearly linear coordination of the Ag4 atom. Four weak bonds with the lengths Ag4–O5 2.667(10) and 2.910(10) Å would complete the Ag4 environment to a very distorted octahedral coordination. A linear silver coordination appears to be the third example among tungstates after the structures of $Ag_8W_4O_{16}$ [61] and $Rb_{9-x}Ag_{3+x}Sc_2(WO_4)_9$ [24] with Ag^{II}–O 2.20 Å and 2.13–2.17 Å, respectively. Similar bond lengths Ag–O 2.13–2.22 Å for AgO_2 dumbbells were found also in the structures of $Ag_2Cu_2O_3$ [62] and $[Ag_2M(Te_2O_5)_2]SO_4$ (M = Ce, Th) [63]. The atoms Rb1 and Rb2 have 9-fold environments with the distances Rb1–O 2.934(8)−3.331(10 Å (mean 3.151 Å), Rb2–O 2.993(9)−3.061(9) Å (mean 3.033 Å) and coordination polyhedra as a tricapped octahedron (more exactly, a nearly regular tridiminished icosahedron) and a tricapped trigonal prism, respectively, while the Rb3 has CN = 8 with a tetragonal antiprismatic oxygen environment and Rb3–O 2.961(10)−3.093(9) Å (mean 3.029 Å). The total distances Rb–O fall in the range of the bond lengths observed in the literature for CN (Rb) = 8 and 9 [64].

3.4. Rietveld refinement of $Rb_7Ag_5Sc_2(MoO_4)_9$ structure

All PXRD pattern peaks of $Rb_7Ag_5Sc_2(MoO_4)_9$ were indexed in a rhombohedral unit cell with the parameters close to $Rb_7Ag_5Sc_2(WO_4)_9$ and $Cs_7Na_5Yb_2(MoO_4)_9$ (sp. gr. $R32$). The positional atomic parameters of the $Rb_7Ag_{4.61}Sc_{2.13}(WO_4)_9$ structure were taken as starting model for Rietveld refinement. Refinement was stable and gave low R-factors (Table 2, Fig. 4). The atomic coordinates and main bond lengths are in Tables 3S and 4S, respectively.

3.5. Crystal chemistry of $Rb_7Ag_5Sc_2(XO_4)_9$ (X = W, Mo)

The characteristic details of the title compounds and isostructural $Cs_7Na_5Yb_2(MoO_4)_9$ [57] are 'lanterns' $[M_2(TO_4)_9]$ (M is an octahedral cation, TO_4 is a tetrahedral oxoanion) composed by two MO_6 octahedra sharing corners with six terminal and three bridging TO_4 tetrahedra. These 'lanterns' can be considered as fragments of 3D frameworks $[M_2(TO_4)_3]_{3\infty}$ in the structures of $Sc_2(WO_4)_3$ [4], $NaZr_2(PO_4)_3$ [26] (the NASICON type), langbeinite $K_2Mg_2(SO_4)_3$ and other related compounds [24]. In the structures of $Rb_7Ag_{5-3x}Sc_{2+x}(XO_4)_9$ (X = W, Mo), each 'lantern' is further strengthened by three AgO_2 dumbbells linked the opposite terminal XO_4 tetrahedra to give isolated building blocks

Table 2
Main parameters of processing and refinement of the $Rb_7Ag_5Sc_2(MoO_4)_9$ sample.

Compound	$Rb_7Ag_5Sc_2(MoO_4)_9$
Sp. gr.	*R*32
a, Å	10.16334 (6)
c, Å	35.5077 (3)
V, Å^3	3176.33 (5)
Z	3
2*θ*-interval, °	7–100
R_{wp}, %	3.70
R_p, %	2.71
R_{exp}, %	1.15
$\chi 2$	3.23
R_B, %	1.02

$[Ag_3M_2(XO_4)_9]$ where M = Sc or (Sc,Ag). These building blocks together with the Rb1 and Rb2 cations form two-story hexagonal layers parallel to (001) plane (Fig. 5, *a*), which resemble the structure motif of glaserite $K_3Na(SO_4)_2$ [43]. The layers are connected by Rb3, (Ag,Sc)1 and Ag3 cations (Fig. 5, *b*) and stack with each other to keep their overall trigonal symmetry.

Similar layers of $[Ag_3Sc_2(WO_4)_9]^{9-}$ clusters parallel to the (001) plane were found by us in the $Rb_{9-x}Ag_{3+x}Sc_2(WO_4)_9$ structure [24], but due to some mutual shift of the layers along this plane the compound symmetry becomes pseudo hexagonal (orthorhombic, the space group *Cmcm*). Thus, the structures of both triple tungstates in the system Rb_2WO_4–Ag_2WO_4–$Sc_2(WO_4)_3$ are based on topologically identical layers of $[Ag_3M_2(WO_4)_9]^{9-\delta}$ clusters but differ in their mutual stacking and the ratio Rb^+/Ag^+ with the equal sum of these cations in the compounds. The same seem to occur in the system Rb_2MoO_4–Ag_2MoO_4–$Sc_2(MoO_4)_3$.

Analogous hexagonal layers of $[M_2(TO_4)_9]$ units were also observed in $Cs_7Na_5Yb_2(MoO_4)_9$ [57] and $Na_{13}Sr_2Ta_2(PO_4)_9$ [65]. In both structures the role of 'bracing' AgO_2 dumbbells play distorted NaO_6 octahedra, while the interlayer space is filled by NaO_6 trigonal prisms and CsO_8 polyhedra in $Cs_7Na_5Yb_2(MoO_4)_9$ or by sodium polyhedra with CN = 5 and 6 in $Na_{13}Sr_2Ta_2(PO_4)_9$. The layers in $Cs_7Na_5Yb_2(MoO_4)_9$ are arranged by the rhombohedral unit cell translations (the space group *R*32), whereas the layers in $Na_{13}Sr_2Ta_2(PO_4)_9$ stack under each other and connected by 6_3 screw axes (the space group $P6_3/m$).

An alternative approach to describe the structures of $Rb_7Ag_{5-3x}Sc_{2+x}(XO_4)_9$ (X = W, Mo), $Cs_7Na_5Yb_2(MoO_4)_9$ and other compounds related to the glaserite, $K_3Na(SO_4)_2$, structure type may be based on their representation as sets of polyhedral rods around all threefold axes, which are connected through common oxygen vertices with bridging TO_4 tetrahedra and other cation polyhedra to form 3D frameworks [66]. In particular, as we showed in Ref. [60], the $Cs_7Na_5Yb_2(MoO_4)_9$ structure type [57] belongs to the series of rhombohedral layered or framework molybdates with $a \approx 9$–10 Å and large *c*-periods (more than 20 Å) where around all three-fold axes there are columns (rods) of coordination polyhedra shared faces with each other or with empty trigonal prisms (Table 3). Such polyhedral rods are linked together with bridged TO_4 tetrahedra to form layered or open 3D framework structures. Thus, the structure of $Cs_7Na_5Yb_2(MoO_4)_9$ may be represented as ten-membered (along the *c* period) columns of NaO_6 and empty trigonal prisms, CsO_9 polyhedra, YbO_6 octahedra in the following sequence: … $[NaO_6]$ (*p*)−CsO_9–CsO_9–NaO_6 (*p*)−YbO_6−[□O_6] (*p*) …, where empty prisms named as □O_6 (*p*). The corresponding column in isostructural $Rb_7Ag_{4.61}Sc_{2.13}(WO_4)_9$ looks as … [(Ag,Sc)1O_6]−Rb2O_9–Rb1O_9–Ag3O_6 (*p*)−(Sc,Ag)2O_6−[□O_6] (*p*) … (Fig. 5, *c*) with taking into account octahedral coordination of the (Sc,Ag)2 site.

It should be noted that a number of the compounds belonging to the considered series of rhombohedral complex molybdates are good cationic conductors, for example, NASICON-like phases. Significant ionic conductivity comparable with that of NASICON-like sodium-ion conductors was also found for $Rb_2AgIn(MoO_4)_3$ [60] from this series. The structures of $Rb_7Ag_5Sc_2(XO_4)_9$ (X = W, Mo), $Rb_{9-x}Ag_{3+x}Sc_2(WO_4)_9$, $Cs_7Na_5Yb_2(MoO_4)_9$ and $Na_{13}Sr_2Ta_2(PO_4)_9$ built on the base of layered arrangement of 'lanterns' $[M_2(TO_4)_9]$ together with presence of cationic vacancies in interlayer space would also be favorable for 2D mixed cation conductivity at the elevated temperatures. So, a positional disorder of the interlayer Rb^+ ions in combination with wide common quadrangular faces of their coordination polyhedra favor to 2D rubidium-ion conductivity in the (001) plane in $Rb_{9-x}Ag_{3+x}Sc_2(WO_4)_9$ that was confirmed with the calculations of bond valence sum (BVS) maps and electrical conductivity measurements [24]. The transport of interlayer Ag^+ or Na^+ cations may be also expected for $Rb_7Ag_{5-3x}Sc_{2+x}(XO_4)_9$ (X = W, Mo), $Cs_7Na_5Yb_2(MoO_4)_9$ and $Na_{13}Sr_2Ta_2(PO_4)_9$ that should draw attention to experimental measurements of their ionic conductivity.

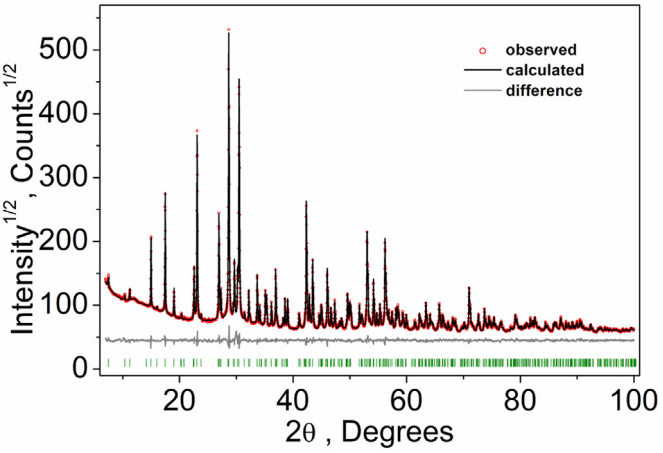

Fig. 4. Observed, calculated and difference diffractograms of $Rb_7Ag_5Sc_2(MoO_4)_9$.

Table 3
Rod representation of some rhombohedral structure types of complex molybdates with $a \approx 9$–10 Å and long *c*-periods[a].

Structure	Sp. gr., *Z*	*a*, Å	*c*, Å	Polyhedral rod
$K_{0.6}(Mg_{0.3}Sc_{0.7})_2(MoO_4)_3$ (NASICON type) [12]	*R*3*c*, 6	9.430	24.337	… ($\underline{K_{0.6}□_{0.4}}$)$\underline{O_6}$−($Sc_{0.7}Mg_{0.3}$)$O_6$−[□$O_6$] (*p*) …
$Cs_7Na_5Yb_2(MoO_4)_9$ [57]	*R*32, 3	10.511	36.358	… [NaO_6] (*p*)−CsO_9–CsO_9–($Na_{0.5}□_{0.5}$)O_6 (*p*)−YbO_6− [□O_6] (*p*) …
$Rb_7Ag_5Sc_2(MoO_4)_9$ (this work)	*R*32, 3	10.163	35.508	… [Ag1O_6]−Rb2O_9–Rb1O_9−($Ag_{0.5}□_{0.5}$)3O_6 (*p*) −ScO_6−[□O_6] (*p*) …
$Rb_7Ag_{4.61}Sc_{2.13}(WO_4)_9$ (this work)	*R*32, 3	10.203	35.427	… [($Ag_{0.69}Sc_{0.31}$)1O_6]−Rb2O_9–Rb1O_9−($Ag_{0.37}□_{0.63}$)3O_6 (*p*)−(Sc,Ag)2O_6−[□O_6] (*p*) …
$K_5(Mg_{0.5}Zr_{1.5})(MoO_4)_6$ [67]	*R*3*c*, 6	10.576	37.511	… ($Zr_{1.5}Mg_{0.5}$)O_6–KO_9−□O_6 (*p*)−($Zr_{1.5}Mg_{0.5}$)O_6−□O_6 (*p*)−KO_9−($Zr_{1.5}Mg_{0.5}$)O_6 …
$K_5Pb_{0.5}Hf_{1.5}(MoO_4)_6$ [68]	*R*3, 6	10.739	37.933	… $\underline{HfO_6}$−□O_6 (*p*)−KO_9–HfO_6–KO_{12}–$\underline{PbO_6}$ …
$Rb_2AgIn(MoO_4)_3$ [60]	*R*3*c*, 12	10.398	38.858	… $\underline{RbO_{12}}$–AgO_6 (*p*)−InO_6−[□O_6] (*p*) …
$Cs_2NaBi(MoO_4)_3$ [69]	*R*3*c*, 12	10.644	40.952	… CsO_{12}−□O_6 (*p*)−BiO_6–NaO_6 (*p*)−BiO_6− NaO_6 (*p*)−CsO_{12} …
$Nd_2Zr_3(MoO_4)_9$ [70]	*R*3*c*, 6	9.804	58.467	… $\underline{ZrO_6}$−□O_6 (*p*)−ZrO_6−□O_6 (*p*)−NdO_9−[□O_6] (*p*) …

[a] Independent parts of polyhedral rods are shown. Centrosymmetric polyhedra are underlined, polyhedra at twofold axes are in square brackets, trigonal prisms are marked with *p* letter. Empty prisms are named as □O_6 (*p*) where □ is a cationic vacancy.

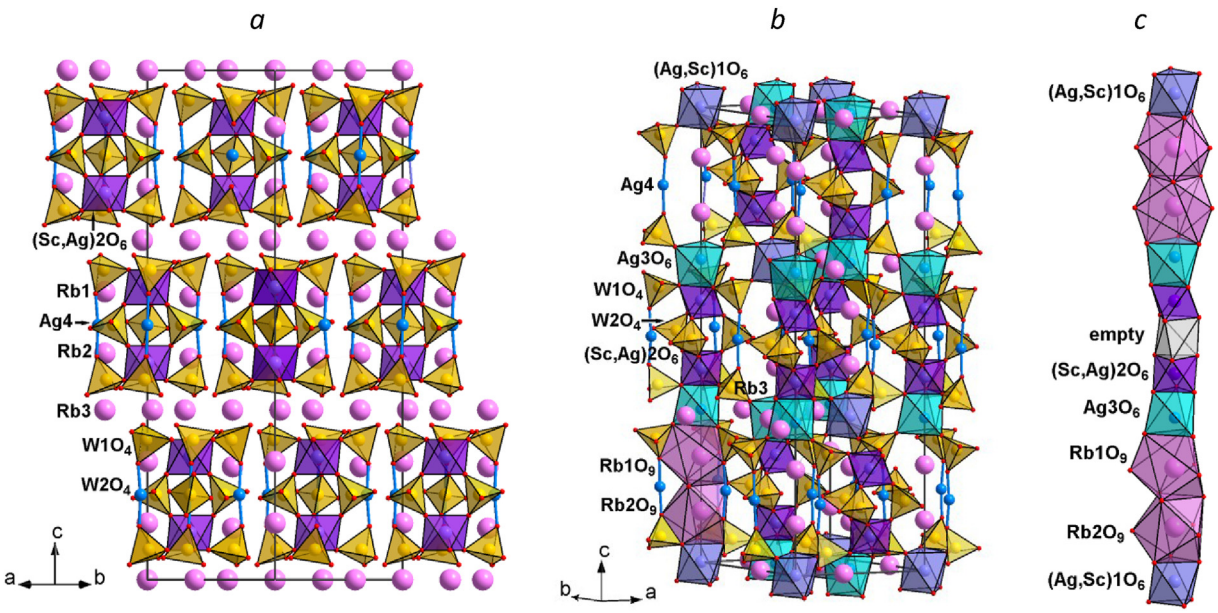

Fig. 5. Crystal structure of $Rb_7Ag_{4.61}Sc_{2.13}(WO_4)_9$: (*a*) layers of $[Ag_3(Sc,Ag)_2(WO_4)_9]^{9-\delta}$ clusters projected on (110); (Ag,Sc)1, (Sc,Ag)2 and Ag3 cations are omitted for clarity; (*b*) a general view in coordination polyhedra of the W, (Ag,Sc)1, (Sc,Ag)2 and Ag3 cations, $Ag4O_2$ dumbbells and Rb spheres; (*c*) a column of face-sharing coordination polyhedra around a threefold the *c* axis.

3.6. SHG and electrical conductivity measurements for $Rb_7Ag_5Sc_2(XO_4)_9$ (X = Mo, W)

Non-centrosymmetricity of $Rb_7Ag_{5-3x}Sc_{2+x}(XO_4)_9$ (X = W, Mo) suggests their nonlinear optical properties, and the presence of cationic vacancies in some silver positions in their structures can contribute to noticeable silver-ion conductivity. Based on these considerations, we conducted studies of the corresponding properties.

The testing results of $Rb_7Ag_5Sc_2(XO_4)_9$ (X = Mo, W) by SHG method ($I_{2\omega}/I_{2\omega}(SiO_2)$ = 0.30 for X = Mo and 0.25 for X = W) are in a good agreement with the acentric space group *R*32, within which the structures of these phases were solved and refinement.

The temperature dependences of electrical conductivity are shown in Fig. 6 in lg(σT) – ($10^3/T$) coordinates. At high temperatures, the conductivity curves do not depend significantly on frequency, with the temperature behavior obeying the Arrhenius law. This is typical for solid electrolytes and can be considered as an indicator of ionic transport in $Rb_7Ag_5Sc_2(XO_4)_9$ (X = Mo, W). The Arrhenius-type linear lg (σT)–($10^3/T$) dependencies are interrupted with step-like discontinuities both on the cooling and heating curves (Fig. 6). Taking into account the significant temperature hysteresis of the phenomenon of about 20–30 K, we associate these phenomena with slightly 'blurred' first-order phase transitions in compounds $Rb_7Ag_5Sc_2(XO_4)_9$ (X = Mo, W).

Electrically conductive properties of ceramics $Rb_7Ag_5Sc_2(XO_4)_9$ (X = Mo, W) were studied by dielectric spectroscopy. Fig. 7, as an example, shows the interdependence of the real and imaginary parts of the complex electrical resistance Z* = Z' + jZ" in the most interesting temperature range near the phase transition in $Rb_7Ag_5Sc_2(MoO_4)_9$ (at temperatures 573, 603, 653, 663, 673 K). The diagram Z"(Z') shown in Fig. 7 has at a temperature of 573 K the typical form of a semicircle for an ionic conductor with the center approximately in the middle between the origin and the intersection point of the semicircle with the Z′ axis. According to the standard approach [71], this indicates the absence of the contribution of electronic conductivity in the substance. The intersection of the abscissa axis by the semicircle falls on the value Z' = $4.2{\cdot}10^4$ Ohm, which, taking into account the geometric dimensions of the sample, corresponds to the specific conductivity of $5.0{\cdot}10^{-3}$ S cm^{-1}, measured at a frequency of 100 Hz at 573 K during the temperature measurements shown in Fig. 6. The obtained agreement allows to expand the comparison of spectroscopic and temperature data to other temperatures, where a semicircle diagram was not obtained due to the limited frequency range of the measuring device (100 Hz–100 kHz). In these cases, the intersection point of the Z′-axis can be determined by extrapolating the ascending branch of the Z"(Z′) diagram at low frequencies to the zero value of Z". In Fig. 7b these data are approximated by straight lines. The points of their intersection with the Z′-axis regularly decrease with increasing temperature, the decreasing values of electric resistivity in Fig. 7b being in good agreement with the increase in conductivity shown in Fig. 6a. Above the phase transition temperatures, the conductivity of the obtained compounds reaches $6.1{\cdot}10^{-3}$ S cm^{-1} (703 K, $Rb_7Ag_5Sc_2(MoO_4)_9$) and $1.4{\cdot}10^{-3}$ S cm^{-1} (733 K, $Rb_7Ag_5Sc_2(WO_4)_9$) with E_a = 0.7 and 0.6 eV, respectively. These values are comparable with typical parameters of ionic conductivity for NASICON-like and similar ionic conductors [17,32].

4. Concluding remarks

Thus, as the main result of studying the subsolidus phase formation in the system Ag_2MoO_4–Rb_2MoO_4–$Sc_2(MoO_4)_3$, two new triple molybdates, $Rb_9Ag_3Sc_2(MoO_4)_9$ and $Rb_7Ag_5Sc_2(MoO_4)_9$, were obtained. The isoformular tungstate analog of the first compound was studied by us earlier and described in Ref. [24], the second compound was synthesized and investigated in this work along with $Rb_7Ag_5Sc_2(WO_4)_9$. The structural study of the latter compound showed a deviation of the studied crystal from stoichiometry, $Rb_7Ag_{4.61}Sc_{2.13}(WO_4)_9$, that can occur at temperatures close to the melting. The same should be expected for the molybdate analog. The acentric compounds $Rb_7Ag_{5-3x}Sc_{2+x}(XO_4)_9$ (X = Mo, W) crystallizing in the chiral space group *R*32 were found to be isostructural to $Cs_7Na_5Yb_2(MoO_4)_9$ and all belong to the series of rhombohedral layered or framework triple molybdates and tungstates with a ≈ 9–10 Å and large *c*-periods (more than 20 Å), many of which have noticeable ionic conductivity at elevated temperatures. It was shown that the structures of both triple tungstates in the system Rb_2WO_4–Ag_2WO_4–$Sc_2(WO_4)_3$, $Rb_7Ag_{5-3x}Sc_{2+x}(WO_4)_9$ and $Rb_{9-x}Ag_{3+x}Sc_2(WO_4)_9$, are based on topologically identical layers of $[Ag_3M_2(WO_4)_9]^{9-\delta}$ clusters but differ in their mutual stacking and the ratio Rb^+/Ag^+ with the equal sum of these cations in the compounds. The same situation seems to occur in the system Rb_2MoO_4–Ag_2MoO_4–$Sc_2(MoO_4)_3$. This stimulates our studies on synthesis, crystal structure determination and

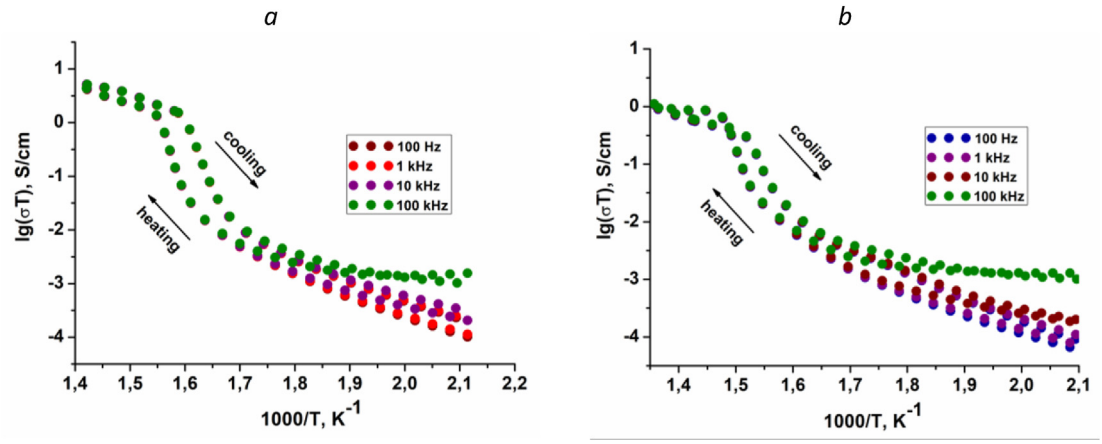

Fig. 6. Temperature dependences of electrical conductivity for $Rb_7Ag_5Sc_2(XO_4)_9$, X = Mo (*a*), W (*b*).

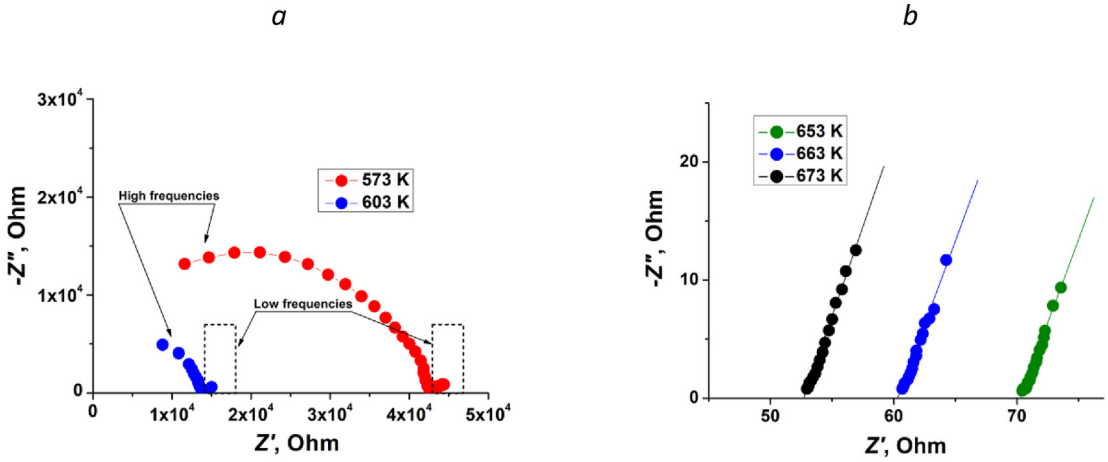

Fig. 7. Diagrams of electrical complex resistivity $Z^* = Z' + jZ''$ for $Rb_7Ag_5Sc_2(MoO_4)_9$ ceramic sample at temperatures below (a) and above (b) phase transition (only for low-frequency branch of the diagram).

measuring electrical conductivity of $Rb_9Ag_3Sc_2(MoO_4)_9$, which are now in progress. It is also of interest to study $Cs_7Na_5Yb_2(MoO_4)_9$, $Na_{13}Sr_2Ta_2(PO_4)_9$, and other related compounds with layers like those found in the structures of $Rb_7Ag_{5-3x}Sc_{2+x}(XO_4)_9$ (X = Mo, W), which could have significant sodium-ion conductivity.

CRediT authorship contribution statement

Tatyana S. Spiridonova: Investigation, Writing – original draft, Visualization, Supervision. **Sergey F. Solodovnikov:** Conceptualization, Structural analysis, Crystallographic description, Writing – review & editing. **Maxim S. Molokeev:** Structure refinement. **Zoya A. Solodovnikova:** Investigation. **Aleksandra A. Savina:** Investigation. **Yulia M. Kadyrova:** Investigation, Visualization. **Aleksandr S. Sukhikh:** Structural analysis. **Evgeniy V. Kovtunets:** Structure refinement. **Elena G. Khaikina:** Conceptualization, Methodology, Writing – review & editing, Funding acquisition.

Declaration of competing interest

The authors declare that they have no known competing financial interests or personal relationships that could have appeared to influence the work reported in this paper.

Acknowledgments

The authors are grateful to Prof. S.Yu. Stefanovich for testing the obtained compounds by the SHG method.

Appendix A. Supplementary data

Supplementary data to this article can be found online at https://doi.org/10.1016/j.jssc.2021.122638.

Funding sources

This research was supported by the Ministry of Science and Higher Education of the Russian Federation, projects No. 0273-2021-0008 (Baikal Institute of Nature Management, SB RAS), and No. 121031700313-8 (Nikolaev Institute of Inorganic Chemistry, SB RAS), as well as partial financial support from the Russian Foundation for Basic Research (project No. № 20-03-00533).

References

[1] J.S.O. Evans, T.A. Mary, A.W. Sleight, Negative thermal expansion in $Sc_2(WO_4)_3$, J. Solid State Chem. 137 (1998) 148–160, https://doi.org/10.1006/jssc.1998.7744.

[2] Y. Zhou, S. Adams, R.P. Rao, D.D. Edwards, A. Neiman, N. Pestereva, Charge transport by polyatomic anion diffusion in $Sc_2(WO_4)_3$, Chem. Mater. 20 (2008) 6335–6345, https://doi.org/10.1021/cm800466y.

[3] A.Ya. Neiman, N.N. Pestereva, Y. Zhou, D.O. Nechayev, E.A. Koteneva, K. Vanec, B. Higgins, N.A. Volkova, I.G. Korchuganova, The nature and the mechanism of ion transfer in tungstates $Me^{2+}\{WO_4\}$ (Ca, Sr, Ba) and $Me^{3+}{}_2\{WO_4\}_3$ (Al, Sc, In) according to the data acquired by the Tubandt method, Russ, J. Electrochem. 49 (2013) 895–907, https://doi.org/10.1134/S1023193512120075.

[4] S.C. Abrahams, J.L. Bernstein, Crystal structure of the transition-metal molybdates and tungstates. II. Diamagnetic $Sc_2(WO_4)_3$, J. Chem. Phys. 45 (1966) 2745–2752.

[5] J.S.O. Evans, T.A. Mary, Structural phase transitions and negative thermal expansion in $Sc_2(MoO_4)_3$, Int. J. Inorg. Mater. 2 (2000) 143–151, https://doi.org/10.1016/S1466-6049(00)00012-X.

[6] B. Zhao, L. Yuan, Sh. Hu, X. Zhang, X. Zhou, J. Tang, Ju. Yang, Controllable synthesis of $Sc_2Mo_3O_{12}$ microcrystals with exposed {001} facets and their remarkable tunable luminescence properties by doping lanthanides, CrystEngComm 18 (2016) 8044–8058, https://doi.org/10.1039/c6ce01640e.

[7] V.A. Isupov, Binary molybdates and tugstates of mono- and trivalent elements as possible ferroelastics and ferroelectrics, Ferroelectrics 321 (2005) 63–90, https://doi.org/10.1080/00150190500259699.

[8] M.B. Zapart, W. Zapart, M. Maczka, Complex ferroelastic domain patterns of $K_{1-x}Rb_xSc(MoO_4)_2$ crystals, Ferroelectrics 497 (2016) 34–41, https://doi.org/10.1080/00150193.2016.1160729.

[9] A.E. Sarapulova, B. Bazarov, T. Namsaraeva, S. Dorzhieva, J. Bazarova, V. Grossman, A.A. Bush, I. Antonyshyn, M. Schmidt, A.M.T. Bell, M. Knapp, H. Ehrenberg, J. Eckert, D. Mikhailova, Possible piezoelectric materials $CsMZr_{0.5}(MoO_4)_3$ (M = Al, Sc, V, Cr, Fe, Ga, In) and $CsCrTi_{0.5}(MoO_4)_3$: structure and physical properties, J. Phys. Chem. 118 (2014) 1763–1773, https://doi.org/10.1021/jp4077245.

[10] X. Ge, X. Liu, Y. Cheng, B. Yuan, D. Chen, M. Chao, J. Guo, J. Wang, E. Liang, Negative thermal expansion and photoluminescence properties in a novel material $ZrScW_2PO_{12}$, J. Appl. Phys. 120 (2016), https://doi.org/10.1063/1.4968546, 205101/1–205101/5.

[11] Y. Cheng, Y. Liang, Y. Mao, X. Ge, B. Yuan, J. Guo, M. Chao, E. Liang, A novel material of $HfScW_2PO_{12}$ with negative thermal expansion from 140 K to 1469 K and intense blue photoluminescence, Mater. Res. Bull. 85 (2017) 176–180, https://doi.org/10.1016/j.materresbull.2016.09.008.

[12] G.J. Wang, Y.S. Huang, L.Z. Zhang, S.P. Guo, G. Xu, Z.B. Lin, G.F. Wang, Growth, structure, and optical properties of the Cr^{3+}:$K_{0.6}(Mg_{0.3}Sc_{0.7})_2(MoO_4)_3$ crystal, Cryst. Growth Des. 11 (2011) 3895–3899, https://doi.org/10.1021/cg200438p.

[13] N.M. Kozhevnikova, S.Y. Batueva, R.M. Gadirov, Luminescence properties of Eu^{3+}-doped $K_{1-x}Mg_{1-x}Sc(Lu)_{1+x}(MoO_4)_3$ ($0 \le x \le 0.5$) solid solutions, Inorg. Mater. 54 (2018) 460–465, https://doi.org/10.1134/S0020168518050072.

[14] N.M. Kozhevnikova, S.Yu. Batueva, Synthesis of a $LiZnSc(MoO_4)_3$:Eu^{3+} – based red phosphor, Inorg. Mater. 55 (2019) 59–63, https://doi.org/10.1134/S0002016859010060.

[15] N.M. Kozhevnikova, M.V. Mokhosoev, Triple Molybdates, Ulan-Ude: Buryatsk, Gos. Univ., Ulan-Ude, 2000 (In Russ.).

[16] N.M. Kozhevnikova, S.Y. Tsyretarova, Synthesis and study of the phase formation in the Na_2MoO_4–$MgMoO_4$–$Sc_2(MoO_4)_3$ system, Russ. J. Inorg. Chem. 60 (2015) 520–525, https://doi.org/10.1134/S0036023615040087.

[17] I.Y. Kotova, D.A. Belov, S.Y. Stefanovich, $Ag_{1-x}Mg_{1-x}R_{1+x}(MoO_4)_3$ Ag^+-conducting nasicon-like phases, where R = Al or Sc and $0 \le x \le 0.5$, Russ. J. Inorg. Chem. 56 (2011) 1189–1193, https://doi.org/10.1134/S0036023611080122.

[18] N.M. Kozhevnikova, S.Y. Batueva, Vibrational spectra and electrophysical properties of $Li_{0.2}K_{0.8-y}Mg_{1-x}Sc(Lu)_{1+x}(MoO_4)_3$ ($0 \le x \le 0.5$, $0 \le y \le 0.3$) solid solutions with a NASICON structure, Russ. J. Inorg. Chem. 63 (2018) 809–814, https://doi.org/10.1134/S0036023618060165.

[19] A.A. Savina, S.F. Solodovnikov, D.A. Belov, Z.A. Solodovnikova, S.Yu. Stefanovich, B.I. Lazoryak, E.G. Khaikina, New alluaudite-related triple molybdates $Na_{25}Cs_8R_5(MoO_4)_{24}$ (R = Sc, In): synthesis, crystal structures and properties, New J. Chem. 41 (2017) 5450–5457, https://doi.org/10.1039/c7nj00202e.

[20] N.I. Medvedeva, A.L. Buzlukov, A.V. Skachkov, A.A. Savina, V.A. Morozov, Ya.V. Baklanova, I.E. Animitsa, E.G. Khaikina, T.A. Denisova, S.F. Solodovnikov, Mechanism of sodium-ion diffusion in alluaudite-type $Na_5Sc(MoO_4)_4$ from NMR experiment and ab initio calculations, J. Phys. Chem. C 123 (2019) 4729–4738, https://doi.org/10.1021/acs.jpcc.8b11654.

[21] A.L. Buzlukov, I.Yu Arapova, Ya.V. Baklanova, N.I. Medvedeva, T.A. Denisova, A.A. Savina, B.I. Lazoryak, E.G. Khaikina, M. Bardet, Coexistence of three types of sodium motion in double molybdate $Na_9Sc(MoO4)6$: ^{23}Na and ^{45}Sc NMR data and ab initio calculations, Phys. Chem. Chem. Phys. 22 (2020) 144–154, https://doi.org/10.1039/c9cp05249f.

[22] J.G. Bazarova, A.V. Logvinova, B.G. Bazarov, Yu.L. Tushinova, S.G. Dorzhieva, J. Temuujin, Synthesis of new triple molybdates $K_5RZr(MoO_4)_6$ (R = Al, Cr, Fe, In, Sc) in the K_2MoO_4–$R_2(MoO_4)_3$–$Zr(MoO_4)_2$ systems, their structure and electrical properties, J. Alloys Compd. 741 (2018) 834–839, https://doi.org/10.1016/j.jallcom.2018.01.208.

[23] V.G. Grossman, J.G. Bazarova, M.S. Molokeev, B.G. Bazarov, New triple molybdate $K_5ScHf(MoO_4)_6$: synthesis, properties, structure and phase equilibria in the M_2MoO_4–$Sc_2(MoO_4)_3$–$Hf(MoO_4)_2$ (M = Li, K) systems, J. Solid State Chem. 283 (2020) 121143, https://doi.org/10.1016/j.jssc.2019.121143.

[24] T.S. Spiridonova, S.F. Solodovnikov, A.A. Savina, Yu.M. Kadyrova, Z.A. Solodovnikova, V.N. Yudin, S.Yu. Stefanovich, I.Yu. Kotova, E.G. Khaikina, V.Yu. Komarov, $Rb_{9-x}Ag_{3+x}Sc_2(WO_4)_9$: a new glaserite-related structure type, rubidium disorder, ionic conductivity, Acta Crystallogr. B 76 (2020) 28–37, https://doi.org/10.1107/S2052520619015270.

[25] R.F. Klevtsova, P.V. Klevtsov, Synthesis and crystal structure of double molybdates $KR(MoO_4)_2$ for R^{3+} = Al, Sc and Fe and tungstate $KSc(WO_4)_2$, Kristallografija 15 (1970) 953–959 (In Russ.).

[26] H.Y.-P. Hong, Crystal structures and crystal chemistry in the system $Na_{1+x}Zr_2Si_xP_{3-x}O_{12}$, Mater. Res. Bull. 11 (1976) 173–182.

[27] S.C. Abrahams, Crystal structure of the transition-metal molybdates and tungstates, J. Chem. Phys. 46 (1967) 2052–2065, https://doi.org/10.1063/1.1841001.

[28] P.B. Moore, Crystal chemistry of the alluaudite structure type: contribution to the paragenesis of pegmatite phosphate giant crystals, Am. Mineral. 56 (1971) 1955–1975.

[29] F. D'Yvoire, E. Bretey, G. Collin, Crystal structure, non-stoichiometry and conductivity of II-$Na_3M_2(AsO_4)_3$ (M = Al, Ga, Cr, Fe), Solid State Ionics 28–30 (1988) 1259–1264, https://doi.org/10.1016/0167-2738(88)90367-0.

[30] B.G. Bazarov, R.F. Klevtsova, A.D. Tsyrendorzhieva, L.A. Glinkaaya, Zh.G. Bazarova, Crystalline structure of triple molybdate $Rb_5FeHf(MoO_4)_6$ – a new phase in the system Rb_2MoO_4–$Fe_2(MoO_4)_3$–$Hf(MoO_4)_2$, J. Struct. Chem. 45 (2004) 993–998, https://doi.org/10.1007/s10947-005-0091-9.

[31] B.G. Bazarov, Ts.T. Bazarova, K.N. Fedorov, Zh.G. Bazarova, R.F. Klevtsova, L.A. Glinskaya, Synthesis and crystal structure of triple molybdate $K_5InHf(MoO_4)_6$, Russ, J. Inorg. Chem. 50 (2005) 1240–1243.

[32] A.V. Astafyev, A.A. Bosenko, V.I. Voronkova, M.A. Krasheninnikova, S.Y. Stefanovich, V.K. Yanovsky, Dielectric, optical properties and ionic conductivity of $TlNbWO_6$ and $RbNbWO_6$ crystals, Kristallografiya 31 (1986) 968–973 (In Russ.).

[33] ICDD PDF-2 Data Base, Cards ## 00-008-0473, 00-034-0061, 00-024-0958, 01-073-2342, 01-072- 2078, 01-089-4691.

[34] V.A. Efremov, A.R. Gizhinsky, V.K. Trunov, Synthesis of single crystals of some double molybdates with a structure derived from the structure of palmyerite, Kristallografija 20 (1975) 138–141 (in Russ.).

[35] Ju.M. Kadyrova, S.F. Solodovnikov, Z.A. Solodovnikova, O.M. Basovich, T.S. Spiridonova, E.G. Khaikina, New double molybdate of silver-rubidium, Vestn. Buryats. Gos. Univ. Khim. Fiz. 3 (2015) 21–25 (In Russ.).

[36] Bruker AXS TOPAS V4, General Profile and Structure Analysis Software for Powder Diffraction Data. User's Manual, Bruker AXS, Karlsruhe, Germany, 2008.

[37] Bruker APEX3 V2018.7-2, Bruker Advanced X-ray Solutions, Madison, Wisconsin, USA.

[38] O.V. Dolomanov, L.J. Bourhis, R.J. Gildea, J.A.K. Howard, H. Puschmann, OLEX2: a complete structure solution, refinement and analysis program, J. Appl. Crystallogr. 42 (2009) 339–341, https://doi.org/10.1107/S0021889808042726.

[39] G.M. Sheldrick, Shelxt – integrated space-group and crystal-structure determination, Acta Crystallogr. A 71 (2015) 3–8, https://doi.org/10.1107/S2053273314026370.

[40] G.M. Sheldrick, Crystal structure refinement with SHELXL, Acta Crystallogr. C 71 (2015) 3–8, https://doi.org/10.1107/S2053229614024218.

[41] N.G. Dorbakov, O.V. Baryshnikova, V.A. Morozov, A.A. Belik, Y. Katsuya, M. Tanaka, S.Yu. Stefanovich, B.I. Lazoryak, Tuning of nonlinear optic and ferroelectric properties via the cationic composition of $Ca_{9.5-1.5x}Bi_xCd(VO_4)_7$ solid solutions, Mater. Des. 116 (2017) 515–523, https://doi.org/10.1016/j.matdes.2016.11.107.

[42] S.K. Kurtz, T.T. Perry, A powder technique for the evaluation of nonlinear optical materials, J. Appl. Phys. 39 (1968) 3798–3812, https://doi.org/10.1063/1.1656857.

[43] K. Okada, J. Ossaka, Structures of potassium sodium sulphate and tripotassium sodium disulphate, Acta Crystallogr. 36 (1980) 919–921, https://doi.org/10.1107/S0567740880004852.

[44] A.A. Evdokimov, V.A. Efremov, V.K. Trunov, I.A. Kleinman, B.F. Dzhurinsky, Compounds of Rare Earth Elements. Molybdates, Tungstates, M.: Nauka, 1991 (In Russ.).

[45] P.V. Klevtsov, R.F. Klevtsova, Polymorphism of mono- and trivalent metals double molybdates and tungstates of composition $M^+R^{3+}(\exists O_4)_2$, Zh. Strukt. Khim. 18 (1977) 419–439 (In Russ.).

[46] B.I. Lazoryak, V.A. Efremov, About double molybdates $Me_5TR(MoO_4)_4$, Kristallografija 32 (1987) 378–384 (In Russ.).

[47] Yu.A. Velikodnyi, V.K. Trunov, Double molybdates and tungstates of indium and scandium with alkali metals, Zh. Neorg. Khim. 22 (1977) 1496–1498 (In Russ.).

[48] P.V. Klevtsov, R.F. Klevtsova, A.V. Demenev, Double rubidium molybdates and tungstates of scandium and indium and potassium-indium tungstate crystallizing in the structural types $KAl(MoO_4)_2$ and $KIn(MoO_4)_2$, Kristallografija 17 (1972) 545–551 (In Russ.).

[49] V.A. Balashov, M.P. Slisskaya, L.S. Zevin, Z.K. Zolina, A.A. Majer, Crystal structure of double molybdates and tungstates of alkali metals (K, Rb, Cs) and scandium, Kristallografija 17 (1972) 1245–1246 (In Russ.).

[50] V.A. Balashov, A.A. Majer, Double molybdates and tungstates of rubidium and cesium with scandium, Izv. AN SSSR. Neorg. Mater. 7 (1971) 822–827 (In Russ.).

[51] M. Wierzbicka-Wieczorek, U. Kolitsch, E. Tillmanns, Crystal chemistry and topology of Rb–M^{III} molybdates (M = Fe, Sc, In) and triclinic $Rb_2Mo_4O_{13}$: novel building blocks, decorated chains and layers, Z. Kristallogr. 224 (2009) 151–162, https://doi.org/10.1524/zkri.2009.1024.

[52] H.G. Bachmann, W. Kleber, Die Struktur des Palmierits und ihre isotypie Beziehungen, Fortschr. Mineral. 31 (1952) 9–11.

[53] P.V. Klevtsov, A.P. Perepelitsa, Double molybdates $AgR^{3+}(MoO_4)_2$ (R = Sc, Fe, Cr), Zh. Neorg. Khim. 29 (1984) 2261–2265 (In Russ.).

[54] R.F. Klevtsova, P.V. Klevtsov, Synthesis of crystals, thermal stability and crystal structure of sodium-indium molybdate $NaIn(MoO_4)_2$, Kristallografija 17 (1972) 955–959 (In Russ.).

[55] W. Guertler, Zur Fortentwicklung der Konstitutionsforschungen bei ternären Systemen, Z. Anorg. Allg. Chem. 154 (1926) 439–455.
[56] A.M. Zakharov, Phase Diagrams of Binary and Ternary Systems, Metallurgiya, Moscow, 1978 (in Russ.).
[57] O.M. Basovich, A.A. Uskova, S.F. Solodovnikov, Z.A. Solodovnikova, E.G. Khaikina, Phase formation in the systems Na_2MoO_4–Cs_2MoO_4–$Ln_2(MoO_4)_3$ and the crystal structure of the new ternary molybdate $Cs_7Na_5Yb_2(MoO_4)_9$, 2011, Vestn. Buryats. Gos. Univ. Khim. Fiz. 3, 24–29. (In Russ.).
[58] G.D. Tsyrenova, S.F. Solodovnikov, E.G. Khaikina, E. T Khobrakova, ZhG. Bazarova, Z.A. Solodovnikova, Phase formation in the systems Ag_2MoO_4-MO-MoO_3 (M = Ca, Sr, Ba, Pb, Cd, Ni, Co, Mn) and crystal structures of $Ag_2M_2(MoO_4)_3$ (M = Co, Mn), J. Solid State Chem. 177 (2004) 2158–2167, https://doi.org/10.1016/j.jssc.2004.01.02.
[59] E.T. Khobrakova, V.A. Morozov, S.S. Khasanov, G.D. Tsyrenova, E.G. Khaikina, O.I. Lebedev, G. Van Tendeloo, B.I. Lazoryak, New molybdenum oxides $Ag_4M_2Zr(MoO_4)_6$ (M = Mg, Mn, Co, Zn) with a channel-like structure, Solid State Sci. 7 (2005) 1397–1405, https://doi.org/10.1016/j.solidstatesciences.2005.08.010.
[60] T.S. Spiridonova, S.F. Solodovnikov, A.A. Savina, Yu.M. Kadyrova, Z.A. Solodovnikova, V.N. Yudin, S.Yu. Stefanovich, E.G. Khaikina, New triple molybdate $Rb_2AgIn(MoO_4)_3$: synthesis, framework crystal structure and ion-transport behaviour, Acta Crystallogr. C 74 (2018) 1603–1609, https://doi.org/10.1107/S2053229618014717.
[61] P.M. Skarstad, S. Geller, $(W_4O_{16})^{8-}$ polyion in the high temperature modification of silver tungstate, Mater. Res. Bull. 10 (1975) 791–800.
[62] P. Gómez-Romero, E.M. Tejada-Rosales, M.R. Palacín, $Ag_2Cu_2O_3$: the first silver copper oxide, Angew. Chem. Int. Ed. 38 (1999) 524–525, https://doi.org/10.1002/(SICI)1521-3773(19990215)38:4<524::AID-ANIE524>3.0.CO;2-F.
[63] T.N. Poe, F.D. White, V. Proust, E.M. Villa, M.J. Polinski, $[Ag_2M(Te_2O_5)_2]SO_4$ (M = Ce^{IV} or Th^{IV}): a new purely inorganic d/f-heterometallic cationic material, Inorg. Chem. 57 (2018) 4816–4819, https://doi.org/10.1021/acs.inorgchem.8b00504.
[64] O.C. Gagné, F.C. Hawthorne, Bond-length distributions for ions bonded to oxygen: alkali and alkaline-earth metals, Acta Crystallogr. B 72 (2016) 602–625, https://doi.org/10.1107/S2052520616008507.
[65] J. Zhao, D. Zhao, Y. Xue, Q. Zhong, S. Zhang, B. Liu, Novel tantalum phosphate $Na_{13}Sr_2Ta_2(PO_4)_9$: synthesis, crystal structure, DFT calculations and Dy^{3+}-activated fluorescence performance, Acta Crystallogr. C 74 (2018) 1045–1052, https://doi.org/10.1107/S2053229618011877.
[66] P.B. Moore, Complex crystal structures related to glaserite, $K_3Na(SO_4)_2$: evidence for very dense packings among oxysalts, Bull. Mineral. 104 (1981) 536–547, https://doi.org/10.3406/bulmi.1981.7504.
[67] R.F. Klevtsova, Zh.G. Bazarova, L.A. Glinskaya, V.I. Alekseev, S.I. Arkhincheeva, B.G. Bazarov, P.V. Klevtsov, K.N. Fedorov, Synthesis of ternary molybdates of potassium, magnesium, zirconium and the structure $K_5(Mg_{0.5}Zr_{1.5})(MoO_4)_6$, J. Struct. Chem. 35 (1994) 286–290.
[68] B.G. Bazarov, R.F. Klevtsova, A.E. Sarapulova, K.N. Fedorov, L.A. Glinskaya, Zh.G. Bazarova, Synthesis and crystal structure of ternary molybdate compound $K_5Pb_{0.5}Hf_{1.5}(MoO_4)_6$, J. Struct. Chem. 46 (2005) 756–760, https://doi.org/10.1007/s10947-006-0197-8.
[69] A.A. Savina, V.V. Atuchin, S.F. Solodovnikov, Z.A. Solodovnikova, A.S. Krylov, E.A. Maximovskiy, M.S. Molokeev, A.S. Oreshonkov, A.M. Pugachev, E.G. Khaikina, Synthesis, structural and spectroscopic properties of acentric triple molybdate $Cs_2NaBi(MoO_4)_3$, J. Solid State Chem. 225 (2015) 53–58, https://doi.org/10.1016/j.jssc.2014.11.023.
[70] R.F. Klevtsova, S.F. Solodovnikov, Yu.L. Tushinova, B.G. Bazarov, L.A. Glinskaya, Zh.G. Bazarova, A new type of mixed framework in the crystal structure of binary molybdate $Nd_2Zr_3(MoO_4)_9$, J. Struct. Chem. 41 (2000) 280–284. https://link.springer.com/article/10.1007/BF02741593.
[71] J. Ross Macdonald, William R. Kenan, Impedance Spectroscopy: Imphasizing Solid Materials and Systems, Wiley Interscience publication, 1990.